Journal of Applied Sciences

ISSN 1812-5654

science alert

ANSInet
an open access publisher
http://ansinet.com

Journal of Applied Sciences 12 (16): 1746-1749, 2012
ISSN 1812-5654 / DOI: 10.3923/jas.2012.1746.1749

Thermal Properties of Graphane: A Greens Function Approach

[1]M. Antony, [1]N. Lawrence and [2]John Bosco Balaguru Rayappan
[1]Department of Physics, St. Joseph's College (Autonomous), Tiruchirappalli-620 002, Tamil Nadu, India
[2]School of EEE and CeNTAB, SASTRA University, Thanjavur-613 401, Tamil Nadu, India

Abstract: Investigations on the hydrogenation of graphane has gained a significant momentum due to its applications in the fields of hydrogen storage, automobiles, etc. The knowledge on lattice vibrations and hence the thermal properties of hydrogenated graphene (graphane) is important in order to use this material for hydrogen storage applications. This study has reported one of the important thermal properties namely Debye-Waller factor and defect modes of graphane by computing phonon frequency modes by considering atomic interactions up to six neighbors in the frame work of Born von Karman formalism and Green's function approach. The estimated defect modes particularly the localized vibrational modes and the values of Debye-Waller factor for a temperature range of 400 to 1300 K have been reported.

Key words: Graphene, defect modes, Debye-Waller factor, graphane, hydrogenation, phonon frequencies

INTRODUCTION

Graphane is a two-dimensional covalently bonded hydrocarbon in which hydrogen (H) atoms are chemically bound to the carbon (C) atoms on alternate sides of the membrane causing a local buckling of the membrane. Sluiter and Kawazoe (2003) first predicted Graphane (GA) and it was recently rediscovered by Sofo *et al.* (2007). With reference to their prediction, GA "hydrogen atoms are chemically bound to the carbon atoms on alternating sides of the membrane" which causes a "local bucking of the membrane". Flores *et al.* (2009) has recently reported such deformations for small membrane size (<1 nm). In the recent past many experimental (Ao and Peeters, 2010) and theoretical investigations (Karssemeijer and Fasolino, 2011; Flores *et al*., 2009; Tewary and Yang, 2009) have been carried out on the electronic, thermal properties of hydrogenated graphene i.e., graphane due to its applications in the fields of astronomy (Huang *et al*., 2009), nuclear industries (Areou *et al*., 2011) and for designing electronic components (Huang *et al*., 2011). The theoretical insight of the hydrogenation process of graphene helps to predict the electronic properties of graphane based devices (Bang and Chang, 2010; Soriano *et al*., 2010). The lattice thermal properties of GA such as thermal contraction, roughness and heat capacity are reported by Neek-Amal and Peeters (2011). Born von Karman formalism was used to compute the phonon dispersion of graphene by considering first, second and third neighbor interactions (Falkovsky, 2008), first and second neighbor interactions with appropriated constraints (Falkovsky, 2007) using the respective force constant values. However, other lattice vibrations based thermal properties such as defect modes and Debye-Waller factor are not reported so far for this system. Hence, in this study, the theoretically calculated results of defect modes and Debye-Waller factor by considering interactions up to six nearest neighbours are reported.

METHOD OF CALCULATION

In recent experiment, Elias *et al*. (2009) demonstrated the fabrication of GA from a graphene (GE) membrane through hydrogenation which was found to be reversible. Since GA can be derived from GE, as a first step, the phonon frequencies of GE are calculated using Born von Karman formalism considering interactions up to sixth neighbors. The following set of force constants have been assigned for first, second, third, fourth, fifth and sixth neighbor interactions:

- Force constants for first: neighbour interaction — A_1, B_1, A_2, B_2, C_2 and D_2
- Force constants for second: neighbour interaction — A_3, B_3, C_3, D_3, A_4, B_4
- Force constants for third: neighbour interaction — A_5, B_5, A_6, B_6, C_6 and D_6
- Force constants for fourth: neighbour interaction — A_7, B_7, C_7, D_7, A_8, B_8, C_8 D_8, A_9, B_9, C_9 and D_9
- Force constants for fifth: neighbour interaction — A_{10}, B_{10}, C_{10}, D_{10}, A_{11} and B_{11}
- Force constants for sixth: neighbour interaction — A_{12}, B_{12}, C_{12}, D_{12}, A_{13} and B_{13}

Corresponding Author: N. Lawrence, Department of Physics, St. Joseph's College (Autonomous), Tiruchirappalli-620 002, Tamil Nadu, India

With these parameters the dynamical matrix has been constructed and the elements of dynamical matrix D are as follows:

$$D(1,1) = A1\cos 2\pi q_x + 2A_2 \cos q_x \pi \cos\sqrt{3}\pi\, q_y + 4A_3 \cos 3\pi q_x \cos\sqrt{3}\pi\, q_y + 2B_4 \cos 2\, q_y + A_5 \cos 4\,\pi\, q_x + 2A_6 \cos 2\pi q_x \cos 2\sqrt{3}\pi q_y + 2A_7 \cos 5\pi q_x \cos\sqrt{3}\pi q_y + 2A_8 \cos\pi q_x \cos 3\sqrt{3}\pi\, q_y + 2A_9 \cos 4\pi q_x \cos 2\sqrt{3}\pi q_y + 4A_{10} \cos 3\pi q_x \cos 3\sqrt{3}\pi q_y + 2A_{11} - \cos 6\pi qx + 4A_{12} \cos 6\pi q_x \cos 2\sqrt{3}\pi\, q_y + 2B_{13} \cos 4\sqrt{3}\pi q_y \quad (1)$$

$$D(1,2) = -2B_2 \sin\pi\, q_x \sin\sqrt{3}\pi\, q_y - 4B_3 \sin 3\,\pi q_x \sin\sqrt{3}\pi\, q_y - 2B_6 \sin 2\,\pi\, q_x \sin 2\sqrt{3}\pi q_y - 2B_7 \sin 5\pi q_x \sin\sqrt{3}\pi q_y - 2B_8 \sin\pi q_x \sin 3\sqrt{3}\pi q_y - 2B_9 \sin 4\pi q_x \sin 2\sqrt{3}\pi q_y - 4B_{10} \sin 3\pi q_x \sin 3\sqrt{3}\pi q_y - 4B_{12} \sin 6\pi q_x \sin 2\sqrt{3}\pi q_y \quad (2)$$

$$D(1,4) = -A_1 \sin 2\pi q_x + 2A_2 \sin\pi q_x \cos\sqrt{3}\pi qy + A_5 \sin 4\pi q_x - 2A_6 \sin 2\pi q_x \cos 2\sqrt{3}\pi q_y - 2A_7 \sin 5\pi q_x \cos\sqrt{3}\pi q_y + 2B_8 \sin\pi q_x \cos 3\sqrt{3}\pi q_y + 2A_9 \sin 4\pi q_x \cos 2\sqrt{3}\pi q_y \quad (3)$$

$$D(1,5) = 2B_2 \cos\pi q_x \sin\sqrt{3}\pi q_y - 2B_6 \sin 2\sqrt{3}\pi q_y \cos 2\pi q_x - 2B_7 \cos 5\pi q_x \sin\sqrt{3}\pi q_y + 2B_8 \sin 3\sqrt{3}\pi q_y \cos\pi q_x + 2A_9 \sin 2\sqrt{3}\pi q_y \cos 4\pi q_x \quad (4)$$

$$D(2,2) = B_1 \cos 2\pi qx + 2C2 \cos\pi q_x \cos\sqrt{3}\pi q_y + 4C3 \cos 3\pi q_x \cos\sqrt{3}\pi q_y + 2A_4 \cos 2\sqrt{3}\pi q_y + B_5 \cos 4\pi q_x + 2C_6 \cos 2\pi q_x \cos 2\sqrt{3}\pi q_y + 2C_7 \cos 5\pi q_x \sqrt{3}\pi\cos q_y + 2C_8 \cos\pi q_x \cos 3\sqrt{3}\pi q_y + 2C_9 \cos 4\pi q_x \cos 2\sqrt{3}\pi q_y + 4C_{10} \cos 3\pi q_x \cos 3\sqrt{3}\pi q_y + 2B_{11} - \cos 6\pi q_x + 4C_{12} \cos 6\pi q_x \cos 2\sqrt{3}\pi q_y + 2A_{13} \cos 4\sqrt{3}\pi q_y \quad (5)$$

$$D(2,5) = -B_1 \sin 2\pi q_x + 2C_2 \sin\pi q_x \cos\sqrt{3}\pi q_y + B_5 \sin 4\pi q_x - 2C_6 \sin 2\pi q_x \cos 2\sqrt{3}\pi q_y - 2C_7 \sin 5\pi q_x \cos\sqrt{3}\pi q_y + 2C_8 \sin\pi q_x \cos 3\sqrt{3}\pi q_y + 2C_9 \sin 4\pi q_x \cos 2\sqrt{3}\pi q_y \quad (6)$$

$$D(3,3) = B_1 \cos 2\pi q_x + 2D_2 \cos\pi q_x \cos\sqrt{3}\pi q_y + 4D_3 \cos 3\pi q_x \cos\sqrt{3}\pi q_y + 2B_4 \cos 2\sqrt{3}\pi q_y + B_5 \cos 4\pi q_x + 2D_6 \cos 2\pi q_x \cos 2\sqrt{3}\pi q_y + 2D_7 \cos 5\pi q_x \cos\sqrt{3}\pi q_y + 2D_8 \cos\pi q_x \cos 3\sqrt{3}\pi q_y + 2D_9 \cos 4\pi q_x \cos 2\sqrt{3}\pi q_y + 4D_{10} \cos 3\pi q_x \cos 3\sqrt{3}\pi q_y + 2B_{11} - \cos 6\pi q_x + 4D_{12} \cos 6\pi q_x \cos 2\sqrt{3}\pi q_y + 2B_{13} \cos 4\sqrt{3}\pi q_y \quad (7)$$

$$D(3,6) = -B_1 \sin 2\pi q_x + 2D_2 \sin\pi q_x \cos\sqrt{3}\pi q_y + B_5 \sin 4\pi q_x - 2D_6 \sin 2\pi q_x \cos 2\sqrt{3}\pi q_y - 2D_7 \sin 5\pi q_x \cos\sqrt{3}\pi q_y + 2D_8 \sin\pi q_x \cos 3\sqrt{3}\pi q_y + 2D_9 \sin 4\pi q_x \sqrt{3}\pi\cos 2\, q_y \quad (8)$$

D (1, 3) = D (1, 6) = D (2, 3) = D (2, 6) = D (3, 1) =
D (3, 2) = D (3, 4) = D (3, 5) = 0
D (4, 3) = D (4, 6) = D (5, 3) = D (5, 6) = D (6, 1) =
D (6, 2) = D (6, 4) = D (6, 5) = 0
D (2, 1) = D (1, 2) = D (4, 5) = D (5, 4)
D (2, 4) = D (1, 5) =-D (4, 2) =-D (5, 1)
D (4, 1) =-D (1, 4)
D (4, 4) = D (1, 1)
D (5, 2) = -D (2, 5)
D (5, 5) = D (2, 2)
D (6, 3) = -D (3, 6)
D (6, 6) = D (3, 3)

Phonon frequencies and eigenvectors are obtained by diagonalising this matrix for 14 wave vector points obtained by uniformly dividing the Brillouin zone. Using the phonon frequencies and eigenvectors, the greens function values are calculated using the formula:

$$G_{\alpha\beta}\begin{pmatrix} l & l' \\ k & k' \end{pmatrix};\omega^2 = \frac{1}{N\sqrt{m_k m_{k'}}} \sum_{\vec{q}} \frac{e_\alpha(k|\vec{q}\,j) e_\beta^*(k'|\vec{q}\,j)}{\omega_{max}^2} \exp\left[i\vec{q}.\left(\vec{R}(l) - \vec{R}(l')\right)\right] \quad (9)$$

where, ω_{max} is the maximum frequency among all normal modes of the host crystal.

Using these green function values and the change in dynamical matrix due to the presence of hydrogen, the defect modes are calculated by soling the secular equation:

$$|I - g\delta l'| = 0 \quad (10)$$

Debye-Waller factor is calculated using the formula:

$$B = \frac{8\pi^2}{3} < u_1^2 > \quad (11)$$

Where:

$$< u_1^2 > = \frac{1}{2}\int_0^{\infty} \left(\frac{u_1^2}{\omega}\right) \coth\left(\frac{\hbar\omega}{K_B T}\right) dw \quad (12)$$

The u_1 values are calculated using the formula:

$$u_1 = [I + g\partial l' (I - \partial l)^{-1}] u_{0\alpha} \quad (13)$$

Where:

$$u_{0\alpha}\begin{pmatrix} l \\ k \end{pmatrix}; \vec{q}\lambda = \sqrt{\frac{\hbar}{2Nm_k\omega_{q\lambda}}} e_\alpha(k, \vec{q}\lambda) \exp\left(i\vec{q}.r\begin{pmatrix} l \\ k \end{pmatrix}\right) \quad (14)$$

RESULTS AND DISCUSSION

By considering the hexagonal close packed coordinates of the system of study and applying the modified Morse potential (Belytschko *et al.*, 2002), the force constant values were calculated and are listed in Table 1.

Table 1: Force constant values in 10^4 dynes cm^{-2}

Force constant	A_1	B_1	C_2	D_2	A_2	B_2	C_3	D_3
Value	65.1871	1.5599	42.28	1.559	17.4667	29.111	-3.113	0.7281
Force constant	A_3	B_3	C_6	D_6	A_4	B_4	C_7	D_7
Value	-10.796	-5.925	-5.769	0.2419	-14.637	0.7281	-0.119	0.0166
Force constant	A_5	B_5	C_8	D_8	A_6	B_6	C_9	D_9
Value	-7.773	0.2419	-1.205	0.0166	-1.7620	-3.2289	-0.526	0.0166
Force constant	A_7	B_7	C_{10}	D_{10}	A_8	B_8	C_{12}	D_{12}
Value	-1.1146	-0.375	-0.314	0.0039	-0.0286	-0.2185	0.0246	0.0006
Force constant	A_9	B_9	A_{10}	B_{10}	A_{11}	B_{11}	A_{12}	B_{12}
Value	-0.7074	-0.611	-0.102	-0.179	-0.4200	0.0039	-0.075	-0.043
Force constant	A_{13}	B_{13}						
Value	-0.1002	0.0006						

Table 2: The defect modes

Modes (cm^{-1})								
1600.62	1604.33	1606.45	1610.16	1619.71	1629.26	1636.16	1649.42	1656.85
1663.75	1671.71	1672.77	1675.42	1680.20	1683.38	1687.62	1700.89	1707.78
1708.84	1709.90	1716.80	1717.86	1719.45	1724.76	1734.31	1735.37	1741.74
1745.98	1752.35	1762.43	1770.92	1773.57	1786.83	1805.93	1811.77	1813.36
1814.95	1841.48	1847.84	1848.90	1853.15	1871.72	1878.61	1879.68	1894.53
1897.18	1908.85	1915.75	1918.40	1923.71	1926.36	1938.56	1949.71	1952.89
1993.74	2001.70	2003.29	2059.00	2064.83	2066.42	2068.54	2073.32	2076.50
2079.16	2093.48	2105.68	2106.74	2117.35	2124.78	2141.76	2159.80	2170.94
2183.14	2187.91	2195.87	2199.59	2212.85	2226.64	2234.07	2247.33	2251.58
2268.56	2292.43	2304.63	2310.47	2311.53	2326.38	2336.99	2340.71	2343.36
2358.22	2367.23	2370.95	2390.58	2416.04	2425.06	2462.20	2465.38	2465.38
2480.77	2488.73	2523.74	2581.57	2584.22	2584.75	2593.77	2649.48	2674.41
2686.08	2724.28	2762.48	2790.07	2865.40	2963.02	3003.34	3007.06	3101.49
3123.24	3159.85	3190.09	3242.08	3253.75	3320.60	3433.60	3649.53	3742.37
3797.02	3828.32	3943.98	4492.55	4714.84	4942.97	5200.81	5576.42	6182.82

The computed force constant values have been substituted in the dynamical matrix and the phonon frequencies and eigenvectors were calculated by diagonalising the dynamical matrix for 14 representative points obtained by uniformly dividing the Brillouin zone (Balaguru *et al*., 2002).

In the presence of defects, the individual frequency levels inside the bands of allowed frequencies are shifted by small amounts and a small number of frequencies which normally lie near the band edges can emerge out of the allowed bands into the gap of the forbidden frequencies. Such normal modes are called Localised Vibrational Modes (LVM) and they have frequencies greater than the maximum frequency of the host crystal. LVMs are observed due to light impurities or impurities which are tightly bound to the surrounding atoms.

A special kind of LVM has been identified with the characteristic that its frequency, instead of lying above the maximum frequency of the host crystal falls in the gap of the two host crystal frequencies. Such modes are called gap modes. In addition to these two modes, resonance type mode occurs, for which, the vibrational amplitude of defect atom is very much higher compared to that of host crystal atoms.

Greens function approach was adapted to estimate the defect mode present in graphane and calculated resonance and gap modes are given in Table 2. The maximum phonon frequency mode of graphene falls at

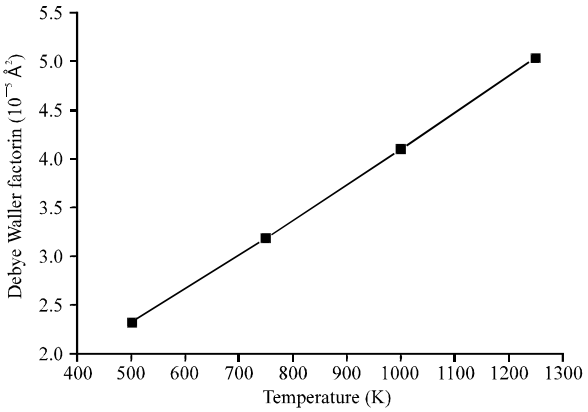

Fig. 1: Debye-Waller factor vs. temperature

1600 cm^{-1} (Maultzsch *et al*., 2002; Zimmermann *et al*., 2008; Mohr *et al*., 2007) and the estimated defect modes after the hydrogenation of graphene falls in the range of 1600.62 to 6182.82 cm^{-1}. Since all these modes are greater than the maximum frequency of the host system, all the listed modes in Table 2 are called as localized vibrational modes.

There are neither other theoretical nor experimental results available to compare our results with them. The computed Debye-Waller factor values were estimated at various temperatures and are shown in Fig. 1. It increases with temperature as expected.

As there are no reported works for GA, the results are compared with that of GE (Tewary and Yang, 2009).

The Debye-Waller factor for GA was found to be much smaller compared to that of GE (Tewary, 2007). This may be due the presence of H in GA and this in-turn generated the defect modes. There are three types of defect modes namely: resonance, gap and localized. Due to the onset of resonance modes, the H atom vibrates with more amplitude by suppressing the amplitude of vibration of the surrounding C atoms. More results in this direction for GA are welcome to check the validity of the present study.

CONCLUSION

The defect modes namely localized vibrational modes, gap modes and resonance modes of Graphane have been computed employing Green's function technique and scattering matrix formalism. This particular study also supports the fact that lattice defects can perturb the thermal properties of low dimensional materials. The computed values of Debye-Waller factor also support the influence of hydrogen induced defect modes in Graphane.

REFERENCES

Ao, Z.M. and F.M. Peeters, 2010. Electric field: A catalyst for hydrogenation of graphene. Applied Phys. Lett., Vol. 96. 10.1063/1.3456384

Areou, E., G. Cartry, J.M. Layet and T. Angot, 2011. Hydrogen-graphite interaction: Experimental evidences of an adsorption barrier. J. Chem. Phys., Vol. 134.

Balaguru, R.J.B., N. Lawrence and S.A.C. Raj, 2002. Lattice Instability of 2H-$TaSe_2$. Int. J. Mod. Phys. B, 16: 4111-4125.

Bang, J. and K.J. Chang, 2010. Localization and one-parameter scaling in hydrogenated graphene. Phys. Rev. B, Vol. 81.

Belytschko, T., S.P. Xiao, G.C. Schatz, R.S. Ruogg, 2002. Atomistic simulations of nanotube fracture. Phys. Rev. B, Vol. 65.

Elias, D.C., R.R. Nair, T.M.G. Mohiuddin, S.V. Morozov and P. Blake *et al*., 2009. Control of Graphene's properties by reversible hydrogenation: Evidence for Graphane. Science, 323: 610-613.

Falkovsky, L.A., 2007. Phonon dispersion in graphene. J. Exp. Theor. Phys., 105: 397-403.

Falkovsky, L.A., 2008. Symmetry constraints on Phonon dispersion in graphene. Phys. Lett. A, 372: 5189-5192.

Flores, M.Z.S., P.A.S. Autreto, S.B. Legoas and D.S. Galvao, 2009. Graphene to graphane: A theoretical study. Nanotechnology, Vol. 20.

Huang, L.F., M.Y. Ni, G.R. Zhang, W.H. Zhou, Y.G. Li, X.H. Zheng and Z. Zeng, 2011. Modulation of the thermodynamic, kinetic and magnetic properties of the hydrogen monomer on graphene by charge doping. J. Chem. Phys., Vol. 135.

Huang, L.F., Y.L. Li, M.Y. Ni, X.L. Wang, G.R. Zhang and Z. Zeng, 2009. Lattice dynamics of hydrogen-substituted graphene systems. Acta Phys. Sin., 58: 306-312.

Karssemeijer, L.J. and A. Fasolino, 2011. Phonons of graphene and graphitic materials derived from the empirical potential LCBOPII. Surf. Sci., 605: 1611-1615.

Maultzsch, J., S. Reich, C. Thomsen, E. Dobardzic, I. Milosevic and M. Damnjanovic, 2002. Phonon dispersion of carbon nanotubes. Solid State Commun., 121: 471-474.

Mohr, M., J. Maultzsch, E. Dobardzic, S. Reich and I. Milosevic *et al*., 2007. Phonon dispersion of graphite by inelastic x-ray scattering. Phys. Rev. B, Vol. 76.

Neek-Amal, M. and F.M. Peeters, 2011. Lattice thermal properties of graphane: Thermal contraction, roughness and heat capacity. Phys. Rev. B, Vol. 83.

Sluiter, M.H.F. and Y. Kawazoe, 2003. Cluster expansion method for adsorption: Application to hydrogen chemisorption on graphene. Phys. Rev. B, Vol. 68.

Sofo, J.O., A.S. Chaudhari and G.D. Barber, 2007. Graphane: A two-dimensional hydrocarbon. Phys. Rev. B, Vol. 75.

Soriano, D., F. Munoz-Rojas, J. Fernandez-Rossier and J.J. Palacios, 2010. Hydrogenated graphenenanoribbons for spintronics. Phys. Rev. B, Vol. 81.

Tewary, V.K. and B. Yang, 2009. Singular behaviour of the Debye-Waller factor of graphene. Phys. Rev. B, Vol. 79.

Tewary, V.K., 2007. Theory of nuclear resonant inelastic x-ray scattering from ^{57}Fe in a single-walled carbon nanotube. Phys. Rev. B, Vol. 75.

Zimmermann, J., P. Pavone and G. Cuniberti, 2008. Vibrational modes and low-temperature thermal properties of graphene and carbon nanotubes: A minimal force-constant model Phys. Rev. B, Vol. 78.